

Nonlinear heat flow in a steadily ablating plasma

T. H. Kho, D. J. Bond, and M. G. Haines

Imperial College of Science and Technology, Blackett Laboratory, London SW7 2BZ, United Kingdom

(Received 25 July 1983)

A simple method of solving the electron-transport equation in the presence of a steadily ablating plasma is described. The results show that, compared with a motionless plasma, the presence of steady-state ablation can substantially reduce the electric field in the direction of the heat flow. It does not lead to further reduction of the (center-of-mass) heat flow.

Heat transport, by electrons in the ablation region of laser-implosion targets is of considerable interest in the design of targets for laser fusion. Comparisons of fluid code simulations with laser-implosion experiments frequently indicate heat flows of up to two orders of magnitude smaller than that given by the classical Spitzer-Harm¹ thermal conductivity, and limited to what appeared to be an anomalously small fraction of its free-streaming value.² One suggestion to account for this apparent inhibition of the heat flow has been that classical transport theory is inappropriate in this region because of its steep temperature gradients and consequent nonlocal effects, and that a more-accurate treatment of electron transport with Coulomb collisions would reveal a much lower heat flow.³ Indeed, in recent years, more-sophisticated kinetic studies of nonlinear heat flow which use the Fokker-Planck equation to describe electron energy transport directly, have revealed heat flows lower by an order of magnitude than that given by the Spitzer-Harm theory.⁴⁻⁶

All these previous studies assumed homogeneous plasma with no ion motion. These restrictions simplified the calculations considerably. In reality, in laser implosions the inward heat flow from the critical surface to the ablation surface is accompanied by an outward acceleration and flow of the ions. The plasma density at the ablation surface is typically two orders of magnitude higher than that at the critical surface (for 1- μ m illumination). An important question is, therefore, how does the inhomogeneity and plasma flow affect the heat flow. The electron pressure gradient that drives the ablation (in a high- Z target) is coupled to the ions by both the electric field and collisions between electrons and ions. The electric field \bar{E} has to satisfy the ion momentum equation (in steady state with one-dimensional planar geometry), $m_i n_i u (\partial u / \partial x) = eE + R_{ie}$, where, m_i , n_i , and u are the mass, density, and flow velocity of the ions, respectively (the ion pressure has been neglected). The last term, R_{ie} , represents the momentum-transfer rate between electrons and ions, which in the absence of a net current is proportional to the thermal gradient. The direction of the electric field must now depend on the relative strength of the collisional and convective terms. In the absence of plasma flow it is everywhere directed inward towards the cooler region, but the inclusion of ion motion could cause it to be directed outwards to accelerate the ions. This would mean that the heated electrons at the critical surface would be accelerated into the ablation region by the electric field instead of being retarded by it, which is the conventional picture. This effect could increase the heat flow (compared to that with no ion motion). On the other hand, transporting the

heated electrons up a density gradient might tend to reduce it. Hence, it is not clear what the net effect of a self-consistent coupling of the electric field, density gradient, and plasma flow is on the heat flow. Of particular interest would be whether the inclusion of ablation could lead to an even lower (center-of-mass) heat flow than that given by the Spitzer-Harm theory.

To gain insight into this problem self-consistent calculations are required. Initial-value kinetic calculations with hydrodynamics are costly to perform. An alternative is to solve directly for the quasi-steady-state. We chose the latter option. Here, we describe a simple method of coupling the electron-transport equation to the hydrodynamics and its results.

Consider a plasma, in planar geometry, steadily ablating from a cold to a hot boundary, corresponding to the ablation and critical surfaces, respectively. The plasma is fully ionized (Al^{13+}), quasineutral, and carries no net current. The electron fluxes entering this ablation region at the hot and cold boundaries are half-Maxwellians with temperatures T_h and T_c , respectively. The mass flux, $m_i n_i u$, carried by the ion flow is constant throughout the ablation region in the steady state. Prescribing the mass flux, T_h , T_c , the density at one of the boundaries, and the separation between these boundaries, specifies the problem completely.

Electron transport is described by the one-dimensional transport equation

$$v_x \frac{\partial f}{\partial x} - eE \frac{\partial f}{\partial v_x} = \left(\frac{\delta f}{\delta t} \right)_{ie}, \quad (1)$$

where f is the electron-distribution function in phase space, x the preferred direction, v the electron speed, E the magnitude of the electric field, and $(\delta f / \delta t)_{ie}$ the electron-ion scattering. This is solved in conjunction with the plasma equation of motion, $m_i n_i u (\partial u / \partial x) = -\partial P / \partial x$, where $P = m_e \int v_x^2 f dv$. Here, m_e is the electronic mass. For simplicity, in the transport equation, electron self-collisions have been ignored. In treating the electron-ion scattering, the ions are assumed to be fixed. This is a reasonable approximation as the plasma flow velocity is of the order of the ion sound speed, $c_x(x)$, which is much smaller than the electron thermal speed v_t [$v_t / u \sim (m_i / m_e) \ll 1$]. Only subsonic flows are allowed: planar geometry cannot support steady supersonic flows. In the equation of motion, the ion pressure is neglected because it is small compared with the electron pressure [$Z = 13$, (ion temperature per electron temperature) ≤ 1].

These equations are solved numerically using two nested

iterations. An inner iteration solves the transport equation for an assumed electric field. Using the electron total energy Q [$Q = \frac{1}{2} m_e v^2 - e\phi(x)$, $\phi(x)$ is the electric potential], and its momentum perpendicular to the direction of the electric field L [$L = m_e v(1 - \mu^2)^{1/2}$, $\mu = v_x/v$] as the independent variables, the transport equation can be expressed as

$$\frac{\partial f}{\partial x} \Big|_{Q,L} = \left(\frac{\delta f}{\delta t} \right)_{ie}$$

Equation (3) can be solved by integrating along trajectories of constant Q and L in phase space. This is done numerically by mapping these trajectories onto an angular mesh across the spatial domain. In the results presented below, 70 of these trajectories (for $0 < \mu < 1$) were used in all the calculations. A diffusionlike moment of the transport equation is used to accelerate convergence. The numerical details of solving the transport equation with this method are to be found in Ref. 7.

The outer iteration searches for the self-consistent electric field to couple the electron and ion motion. The equation of motion which must be satisfied upon convergence is used to correct the electric field according to the formula

$$4\pi \frac{\partial}{\partial x} \int [(Q + e\phi^*) \mu^2 f dv] = -m_i n_i u \frac{\partial u}{\partial x}$$

Here $\phi^*(x)$ is the corrected potential to be used in the next iteration. All the other quantities are evaluated at the current iteration. Convergence is fastest with no ion flow (in which case the electron pressure is constant). The number of outer iterations needed for the simulations presented below ranged from 5 to 20.

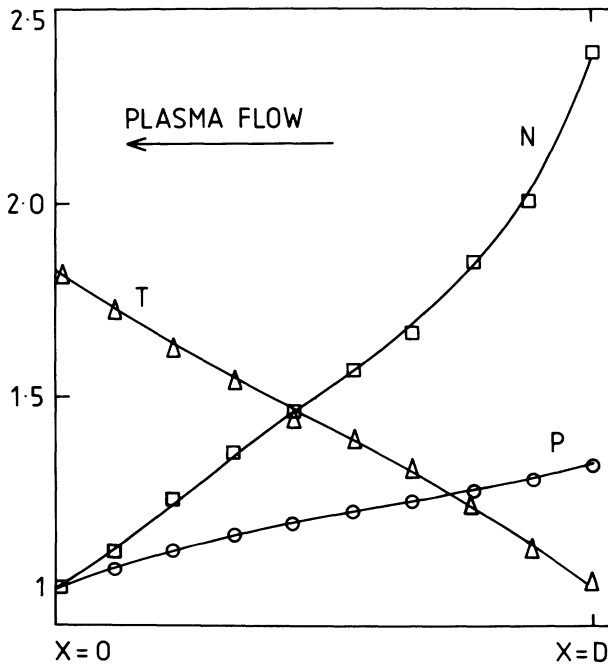


FIG. 1. The electron temperature (T), total electron pressure (P), and density (N) for a simulation with $T_h/T_c=2$ and $D/\bar{\lambda}=10$. The hot boundary is at $X=0$ and the cold boundary, $X=D$. The units are arbitrary.

Calculations were made with $T_h/T_c=2$ for different mass fluxes and system thicknesses parametrized by $D/\bar{\lambda}$, where D is the spatial separation between the boundaries and $\bar{\lambda}$ is the mean free path of an electron at the hot boundary with kinetic energy $\frac{1}{2}k(T_h + T_c)$. Figure 1 illustrates a simulation with $D/\bar{\lambda}=10$ in which the plasma flow attained a Mach number (flow speed per ion sound speed) of 0.74 at the hot boundary. The density, temperature (kinetic), and total electron pressure are shown.

Figure 2 shows the effect of increasing ablating flow on the electronic potential $-e\phi(x)$. For sufficiently high-mass flow the potential becomes nonmonotonic near the hot boundary. The electric field accelerates the ions out of the ablation region near the hot boundary and retards them in the colder, denser region. The reason is as discussed above. In these simulations we have ignored the existence of electrons with total energies less than the escape energy of the potential through and which could, hence, be trapped in it (the total energy is a constant of motion here because of the Lorentz plasma approximation). It is possible that in experiments with high- Z targets some electrons are trapped just behind the critical surface in this way.

Figure 3 shows the normalized heat flow Q/Q_{SP} [calculated center-of-mass heat flow per Spitzer-Harm thermal con-

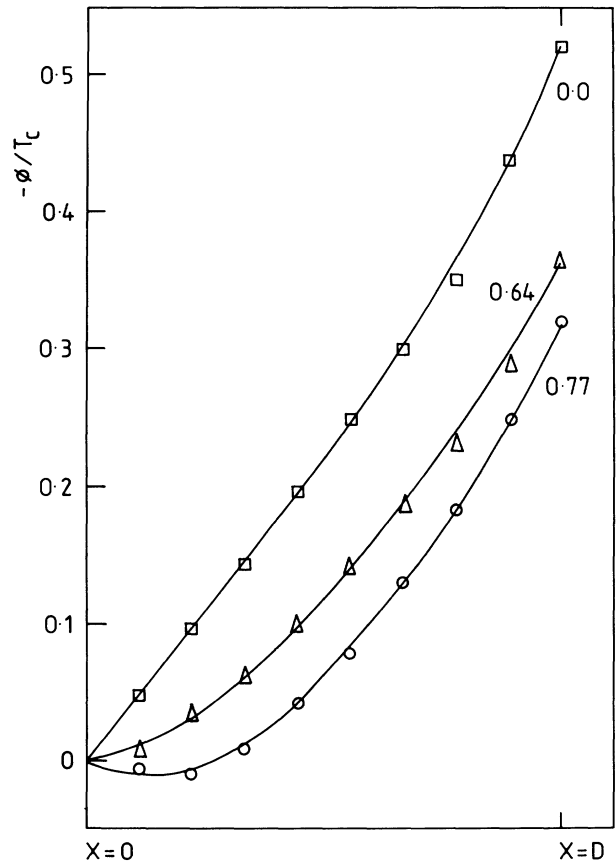


FIG. 2. Effects of increasing steady-state ablation on the electron potential $-e\phi(x)$ along a system with $D/\bar{\lambda}=10$. Each curve represents a simulation with a given (constant) mass flux ($m_i n_i u$) and is labeled by the Mach number the plasma flow attained at the hot boundary ($X=0$). The top curve represents a simulation with no ion motion ($\partial P/\partial x=0$).

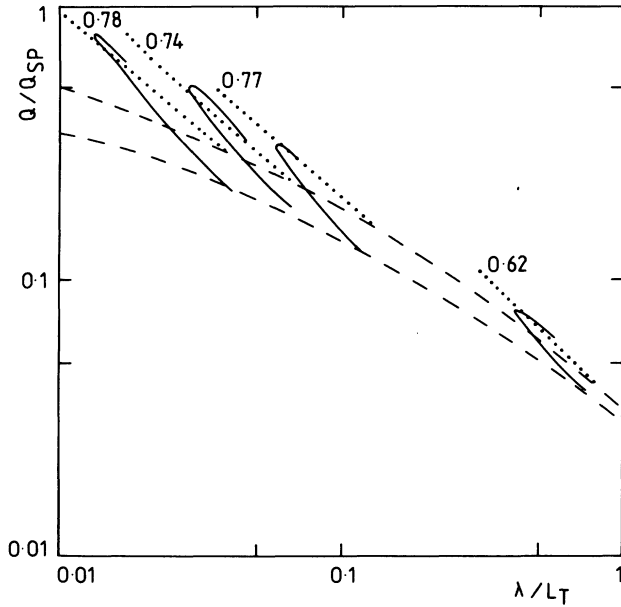


FIG. 3. Comparison of Q/Q_{SP} (calculated heat flow per Spitzer-Harm thermal conduction for a Lorentz plasma evaluated at the local values of λ/L_T). Each solid curve represents Q/Q_{SP} along a system of given D/λ with no ion motion. The effect of including a steady-state ablation in that system is represented by the dotted curve immediately above the bold curve. The dotted curves are labeled by the Mach number the plasma flow attained at the hot boundary ($X=0$). The dashed curves approximate the heat flows at the top of the temperature fronts.

duction evaluated at the local values of (λ/L_T) : λ is the mean free path of an electron with energy $kT(x)$ and L_T is the temperature scale length]. Each bold curve represents Q/Q_{SP} measured along the temperature front in a simulation with no ion motion. The dotted curves represent simulations with ion motion and are labeled by the Mach number the plasma flow attained at the hot boundary. From left to right, each pair of bold and dotted curves corresponds to systems with thicknesses $D/\bar{\lambda}=20, 10, 5$, and

0.5. For all cases, the lowest point of each curve corresponds to that spatial point nearest the hot boundary (critical surface), i.e., at the top of the temperature front. The heat flows can be multivalued in λ/L_T because of nonlocal effects. The high-energy tail of the electrons from the hot boundary streams into the cold region (at the top of the curve) with little attenuation and enhances the heat flow there.

It can be seen that inclusion of steady-state ablation tends to increase Q/Q_{SP} . As the system gets less collisional the difference between the results with and without ion motion decreases. For both cases, in the collisionless limit all macroscopic quantities (including the potential) are constant. The difference between the two cases arises then from the fact that in the fluid frame the flow of the electrons from the hot boundary is shifted inwards with ion motion. For the subsonic flows here, the difference is quite small (Fig. 2, $L_T/\lambda \rightarrow 0$). If there is no ion motion then the electric field in the direction of the heat flow increases as the system becomes more collisional. The inclusion of ion motion does two things, first it reduces this electric field as described above and second it raises the electron pressure gradient to drive it. The increased pressure gradient is affected by a weak smoothing of the temperature profile and a more marked increase in density near the cold boundary. The increased density makes the system more collisional and would tend to lower the heat flow but this effect is not enough to compensate for the lower electric field. Hence, a net increase in the heat flow is seen. As the system gets more collisional, the difference in the electric field with and without steady-state ablation becomes more important. This is reflected in the difference in the heat flows between the two cases with increasing collisionality.

ACKNOWLEDGMENTS

This work was supported by the Science and Engineering Research Council. We thank fellow participants at the 1982 Centre Europeen de Calcul Atomique et Moleculaire Workshop on "The flux-limiter and heat flow instabilities" for useful discussions and Dr. Moser for his hospitality.

¹L. Spitzer and R. Harm, Phys. Rev. **89**, 977 (1953).

²W. L. Kruer, Comments Plasma Phys. Controlled Fusion **5**, 69 (1979).

³M. G. Haines, in *Proceedings of the 20th Scottish Universities Summer School in Laser-Plasma Interactions (1979)*, edited by R. A. Cairns and J. J. Sanderson (Scottish Universities Summer School in Phy-

sics, Edinburgh, 1980).

⁴A. R. Bell, R. G. Evans, and D. J. Nicholas, Phys. Rev. Lett. **46**, 243 (1981).

⁵D. J. Bond, Phys. Lett. **88A**, 144 (1982).

⁶J. P. Matte and J. Virmontt, Phys. Rev. Lett. **49**, 1936 (1982).

⁷D. J. Bond, J. Phys. A **15**, 272 (1982).